ISSN: 2457-502X (https://portal.issn.org/resource/issn/2457-502X) 1583-3186 (https://portal.issn.org/resource/issn/1583-3186)

Impact Factor: 0.650 (https://academic-accelerator.com/Impact-Factor-IF/Revista-Romana-de-Materiale-Romanian-Journal-of-Materials)

H-Index: 11 (https://academic-accelerator.com/H-Index/Revista-Romana-de-Materiale-Romanian-Journal-of-Materials)

SJR Indicator: 0.222 (https://academic-accelerator.com/SJR/Revista-Romana-de-Materiale-Romanian-Journal-of-Materials)

E-MAIL (MAILTO:OFFICE@REVISTA-ROMANA-DE-MATERIALE.RO)
rev.mat[at]upb.ro (mailto:rev.mat@upb.ro)

PHONE (TEL:+40214023835)
+(4) 021 402 38 35 (tel:+40214023835)

ADDRESS (HTTPS://WWW.REVISTA-ROMANA-DE-MATERIALE.UPB.RO/EN/CONTACT/INDEX.PHP#MAP)
1 Gheorghe POLIZU, building I, room 206A, zip code 011061, sector 1, Bucharest (www.revista-romana-de-materiale.upb.ro/en/contact/index.php#map)

+ No. 1

- No. 2

+ Composite fibrous scaffolds designed for bone regeneration

– Effect of elevated temperatures on the properties of nano alumina modified concrete containing zircon sand as fine aggregate

E. H. SUJIONO, M. Y. DAHLAN, A. C. M. SAID, R. A. IMRAN, S. SAMNUR

Abstract

The crystal structure of $Nd_{1.2}FeO_3$ oxide material synthesized by varying calcination temperatures was determined using the X-ray diffraction method. Further analysis by Rietveld refinement using software Rietica showed that all of the samples have an orthorhombic phase structure. The lattice constants of each a sample with variation of calcination temperature is a = 5.581059 ± 0.000736 Å, b = 7.758627 ± 0.000947 Å, c = 5.448341 ± 0.000665 Å; a = 5.580203 ± 0.000695 Å, b = 7.756789 ± 0.000908 Å, c = 5.447646 ± 0.000626 Å; and a = 5.580402 ± 0.000704 Å, b = 7.758957 ± 0.000919 Å, c = 5.449350 ± 0.000634 Å, respectively. The results of lattice constant were associated with the value of Goodness of Fit (GoF) is 0.9101%, 0.8726%, and 0.9303%, respectively. That has a strong indication of a qualified matching between the $NdFeO_3$ model numbers of COD 2003124 with the current experimental results. The value of FWHM and the crystal size of $Nd_{1.2}FeO_3$ samples are 0.22º and 372 nm. The results showed that the variation of calcination temperature has not a significant change in the crystal size and homogeneity of the atomic crystal structure. These results are confirmed by simulation of the atomic structure using the Diamond software, the dominant peak of hkl (121).

Keywords

X-ray diffraction; FWHM; $Nd_{1.2}FeO_3$; Rietveld refinement; Crystal Structure; Morphology

Year

2020

Issue

50 (2)

CRYSTAL STRUCTURE OF $Nd_{1.2}FeO_3$ OXIDE MATERIAL AND ITS RIETVELD REFINEMENT ANALYSIS

E. H. SUJIONO[1] * , M. Y. DAHLAN[1], A. C. M. SAID[1], R. A. IMRAN[1], S. SAMNUR[2]
[1]*Laboratory of Materials Physics, Department of Physics, Universitas Negeri Makassar, Makassar 90224, Indonesia.*
[2]*Department of Mechanical Engineering, Universitas Negeri Makassar, Makassar 90224, Indonesia*

The crystal structure of $Nd_{1.2}FeO_3$ oxide material synthesized by varying calcination temperatures was determined using the X-ray diffraction method. Further analysis by Rietveld refinement using software Rietica showed that all of the samples have an orthorhombic phase structure. The lattice constants of each a sample with variation of calcination temperature is a = 5.581059 ± 0.000736 Å, b = 7.758627 ± 0.000947 Å, c = 5.448341 ± 0.000665 Å; a = 5.580203 ± 0.000695 Å, b = 7.756789 ± 0.000908 Å, c = 5.447646 ± 0.000626 Å; and a = 5.580402 ± 0.000704 Å, b = 7.758957 ± 0.000919 Å, c = 5.449350 ± 0.000634 Å, respectively. The results of lattice constant were associated with the value of Goodness of Fit (GoF) is 0.9101%, 0.8726%, and 0.9303%, respectively. That has a strong indication of a qualified matching between the $NdFeO_3$ model numbers of COD 2003124 with the current experimental results. The value of FWHM and the crystal size of $Nd_{1.2}FeO_3$ samples are 0.22º and 372 nm. The results showed that the variation of calcination temperature has not a significant change in the crystal size and homogeneity of the atomic crystal structure. These results are confirmed by simulation of the atomic structure using the Diamond software, the dominant peak of hkl (121).

Keywords: *X-ray diffraction; FWHM; $Nd_{1.2}FeO_3$; Rietveld refinement; Crystal Structure; Morphology.*

1. Introduction

$NdFeO_3$ compounds which have a perovskite structure with the general formula of $RFeO_3$ (R = Rare-Earth) have investigated its utility in a wide variety of applications such as in solid oxide fuel cells [1], gas sensors [2, 3], the photo-catalysis and catalytic converters [4-6]. $NdFeO_3$ has a perovskite-type orthorhombic structure [7, 8]. In $NdFeO_3$ compounds, there are three main magnetic interactions: Fe-Fe, Nd-Fe, and Nd-Nd [9]. Such interaction competes in determining the structure and properties of attractive magnetic that trigger the number of applications. One of the applications of nanopowders $NdFeO_3$ is a gas sensor to detect H_2S [10] and C_2H_5OH [11]. $NdFeO_3$ oxide material has been successfully synthesized by using various methods, such as hydrothermal [12], combustion [13, 14], sol-gel [15], precipitation method [16] and sonication assisted precipitation [17]. The solid-state reaction is the conventional method is most often used for the synthesis of ceramic compounds [8, 18], in which the process is relatively cheap and easy, and the product of this reaction also has a high purity level and good crystalline compared to the other methods. Authors have experience in the fabrication of such an oxide material, e.g., $YBa_2Cu_3O_y$, NdBaCuO (off-stoichiometric), and $NdFe_xBa_{2-x}Cu_3O_y$, the results have reported elsewhere [19 - 21].

In this research, we reported our current results in the development of NdFeO oxide material as one potential candidate for sensor application. Further analysis is to determine quantitatively the physical characteristics of the material by X-ray diffraction data using Rietveld. Rietveld is a method of matching the theoretical curve with the experimental curve until there is an agreement between the two curves as a whole [22]. Based on this analysis, the crystal quality of materials can be concluded.

$NdFeO_3$ crystal structure is described in the space group Pbnm [23, 24]. Atom is located in crystallographic sites below: Nd_{3+} ion in (4c), Fe_{3+} in (4b) and ion O_2 (4c) and (8d). Fe_{3+} ions are coordinated by six ions O_2 that form octahedral FeO_6. The unit cell is composed of octahedral angle FeO_6 that in which the tilt angle as a function of temperature [25]. In this article, $Nd_{1.2}FeO_3$ synthesized using a solid-state reaction method with variations of calcination temperature. Characterization of material has been done by X-ray diffraction (XRD), which includes phase identification and quantitative analysis using Rietica software, Scanning Electron Microscope (SEM) and Energy Dispersive Spectroscopy (EDS), includes fast EDS mapping.

2.Experimental Procedure

$Nd_{1+x}FeO_3$ oxide material has been grown by using the solid-state method with a variation of molar ratio, sintering temperature, and annealing temperature. The best results with a variety of sintering and annealing temperature are using a molar ratio of x = 0.2 [26]. This current research is reported of synthesis of $Nd_{1.2}FeO_3$ material using raw materials of Nd_2O_3 99.99% purchased by

* Autor corespondent/*Corresponding author*,
E-mail: e.h.sujiono@unm.ac.id

Strem Chemicals-USA and Fe_2O_3 99.99% purchased by Sigma-Aldrich-USA with calcined temperature was varied. Raw materials were mixed using a solid-state reaction method with the molar ratio of x = 0.2. The raw material powder Nd_2O_3 99.99% and Fe_2O_3 99.99% were weighed according to the stoichiometric calculations to get an oxide material $Nd_{1.2}FeO_3$. The mixture of $Nd_{1.2}FeO_3$ that obtained was grinded for 3 hours and calcined at a temperature of 700ºC for 6 hours, then crushed for 5 hours and sintering for 6 hours at a temperature of 950ºC. The synthesis process and the heating then repeated to obtain a better sample homogeneity [8, 27 - 30]. After the samples grinded for 3 hours and repeat to calcinate with variations in temperature 750ºC, 850ºC, and 950ºC, respectively. The product of calcination powder and then grinded back for 5 hours and sintering at a temperature of 950ºC for 6 hours following by cooling down the process until reached of ambient room temperature.

$Nd_{1.2}FeO_3$ powder characterized by X-ray diffraction [Rigaku MiniFlex II, 2θ = 20º - 65º (CuKα, λ = 0.154 nm)] to determine the crystal structure and quantitatively analyzed by Rietveld refinement method using software Rietica. The parameters refined include (1) global parameters: sample displacement and Polynomial background of coefficient function (order of 5) and (2) the parameters phases: the lattice parameters, factor scale, component Gaussian (U), component Gamma (Gam0), asymmetry peak, and preferred orientation. Output parameters used to determine the results of refinement crystallinity and lattice parameters of the samples and the illustration of the atomic structure using the Diamond software.

The analysis of morphology and elemental of the $Nd_{1.2}FeO_3$ powder investigated using FEI Quanta FEG Scanning Electron Microscope (SEM) and Fast Energy Dispersive Spectroscopy (EDS) mapping with magnification 50,000x and 100,000x times.

3.Results and Discussion

3.1 X-Ray Diffraction Analysis

XRD diffraction patterns of oxide material $Nd_{1.2}FeO_3$ powder were synthesized by using the solid-state reaction method with variations of calcination temperature at a temperature of 750ºC, 850ºC, and 950ºC, as shown in Figure 1.

Figure 1 shows the peak of $Nd_{1.2}FeO_3$, and the Nd_2O_3 phase has been identified based on the adjustment of the data using software Match!. This crystallographic curve indicates that the raw materials of Nd_2O_3 and Fe_2O_3 have formed a new $NdFeO_3$ phase. The existence of the formation of a minor Nd_2O_3 phase is an indication that the raw materials are not entirely produced in the $Nd_{1.2}FeO_3$ phase. Imperfection reaction suspected due to the adjustment of calcination temperature, and the heating time is less than optimal. This, according to another study, has explained that the $NdFeO_3$ single phase could be formed with a calcination temperature of 1000ºC and sintered at a temperature of 1200ºC. However, the results obtain defects and also contained cracks [31].

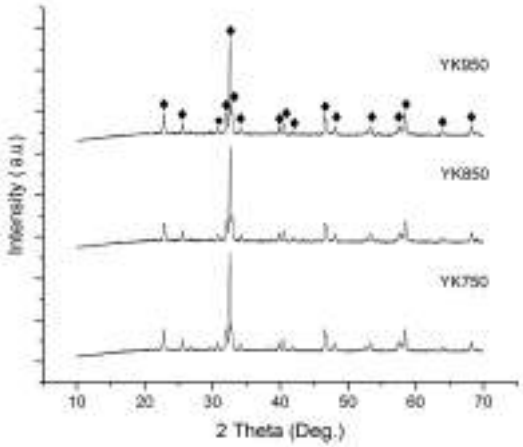

Fig. 1 - XRD pattern of $Nd_{1.2}FeO_3$ as variation of calcination temperature (♦ = $NdFeO_3$, • = Nd_2O_3).

Another researcher, Niu Xinshu et al., also succeeds in synthesized $NdFeO_3$ with a temperature of 950ºC [9] and Yabin Wang et al. with a temperature of 1000ºC [31]. Their results were similar to the current research with the indication of forming the $NdFeO_3$ dominant phase located at 2θ = 32.56º associated with *hkl* value (121). The intensity of the dominant phase of *hkl* (121) increases if the heating temperature is increased [32].

Calculating the crystal size can be estimated by using Debye-Scherer equation as described in Equation (1)

$$D = \frac{0.9\lambda}{\beta cos\theta} \qquad (1)$$

Where λ is the wavelength of the radiation Cu Kα (λ = 0,154 nm), θ is the angle Bragg (º), and β = FWHM at the peak of *hkl* (121) is association 2θ of 32.56º [27]. The calculation results of crystal size and FWHM can be seen in Table 1.

Figure 2 presented the calculation result of the relative intensities as a variation of calcination temperature related to the value of FWHM. The crystal size and homogeneity of surface morphology is no significant change. The existence of the atom due to the Nd_2O_3 phase will reduce the diffraction intensity of each sample. However, the sample with a calcination temperature of 850ºC is shown more dominant at the peak of *hkl* (121). In contrast, it can be seen that the FWHM values for each sample are the same in order of 0.22º. Therefore, the $Nd_{1.2}FeO_3$ oxide material with the dominant peak of hkl 121 and the parameter process, as has explained above, will be useful for the application as gas

Table 1

Data position (2θ), intensity, FWHM, and crystal size of the $Nd_{1.2}FeO_3$ phase

Samples	2θ (°)	Intensity (counts)	FWHM (°)	Crystal size (nm)
YK750	32.56	13063.33	0.22 ± 0.5	372.17 ± 0.02
YK850	32.56	12686.67	0.22 ± 0.5	372.22 ± 0.02
YK950	32.56	13050.00	0.22 ± 0.5	372.17 ± 0.02

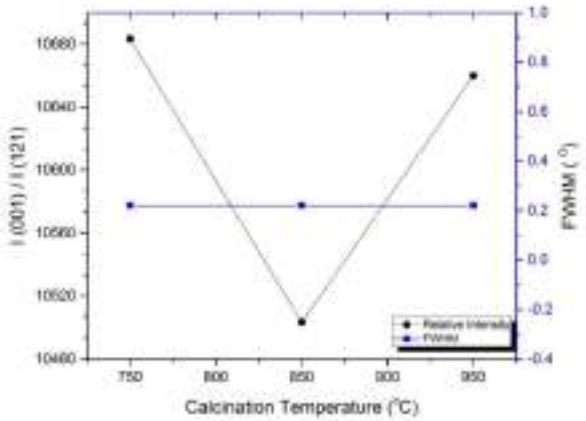

Fig. 2 - The comparison of relative peak intensity and FWHM for the both of phase from three samples $Nd_{1.2}FeO_3$ with the variations of calcination temperature.

Nd_2O_3 number of COD 2002849 [34], while for a $NdFeO_3$ number of COD 2003124 [23].

Figures 3, 4, and 5 show a plot of the results of Rietveld refinement data diffraction of three samples powder $Nd_{1.2}FeO_3$ with the angle of 2θ of 10-70º. The measurable pattern indicated by the sign (+), the calculated pattern shown by the red line, whereas the green line shows the difference between both of them. Suitability (figures-of-merit) of refinement shows in Table 2. The three images formed that the fit between the calculated data and measured data is quite well. There are no other peak differences and plot the difference is not fluctuated significantly, indicating that the Rietveld refinement acceptable under the required criteria, which is the GoF <4% and RWP <20% as was reported Kisi [35]. Other researchers reported compounds $NdFeO_3$ calcined at temperatures of

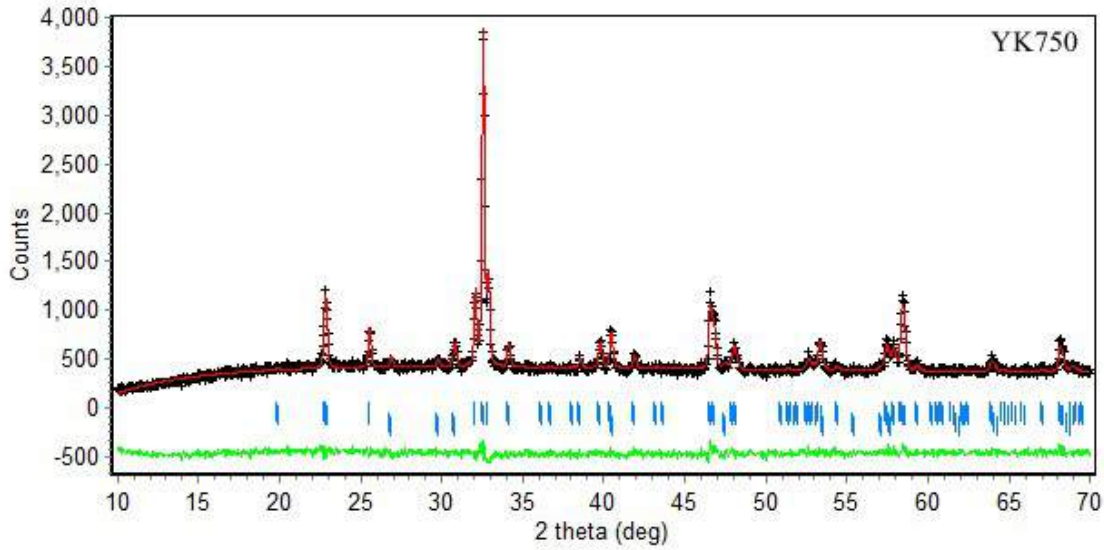

Fig. 3 - The plot of the Rietveld refinement results by using Rietica for sample YK750 oxide material $Nd_{1.2}FeO_3$ in the range 2θ of 10-70º.

sensors as has reported elsewhere [2,3,10,11] for the fast detection of ethanol, propylene, NO_2, CO, C_3H_8, and C_6H_{14}. This result is similar, as has reported [33], FWHM for each peak in the orthorhombic phase has smaller with increasing heating temperature.

3.2. Rietveld Refinement Analysis

In this research, models made from the data COD corresponding to the materials used, for a 750ºC to obtain orthorhombic structure (Pnma) by using the sol-gel route technique, with refinement parameter Rietveld Rp = 8.6, RWP = 6.1, and Goodness of Fit (GoF) = 1.6 [36].

The output of Rietveld refinement analysis showed that the crystal structure of the material of $Nd_{1.2}FeO_3$ is orthorhombic with space group is Pnma, a ≠ b ≠ c, α = β = γ = 90° to the respective lattice parameters are presented in Table 3. This result is comparable with has reported other researchers that synthesize $NdFeO_3$ using sol-gel

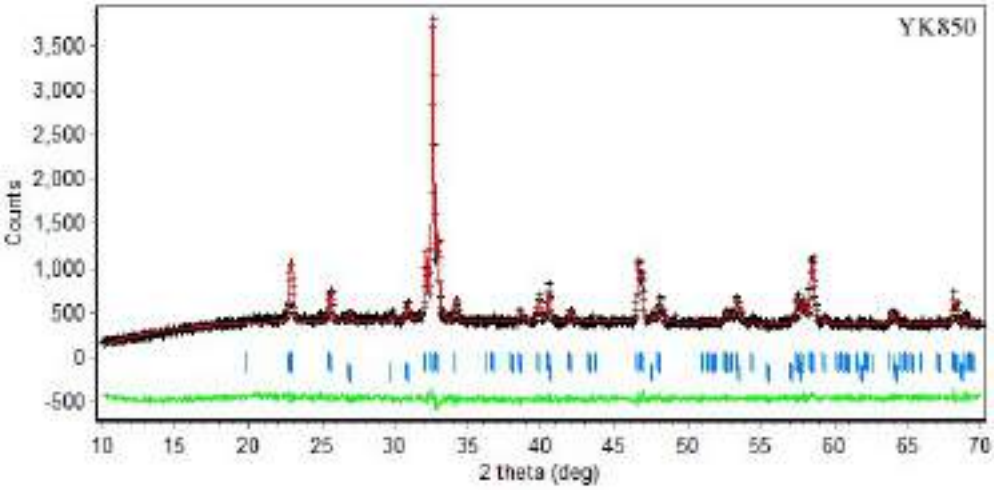

Fig. 4 - The plot of the results Rietveld refinement by using Rietica for sample YK850 oxide material $Nd_{1.2}FeO_3$ in the range 2θ of 10-70º.

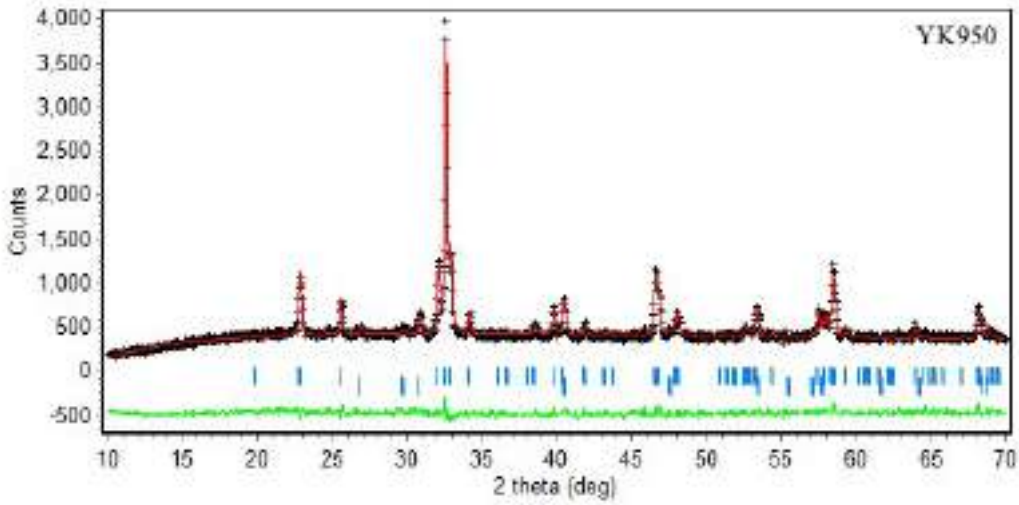

Fig. 5 - The plot of the results Rietveld refinement by using Rietica for sample YK950 oxide material $Nd_{1.2}FeO_3$ in the range 2θ of 10-70º.

method citrate obtained $NdFeO_3$ phase with orthorhombic structure (Pnma) with the lattice parameters is a = 5.578 Å, b = 7.758 Å, c = 5.448 Å [32].

Table 4 is the weight percentage of each phase, the highest weight percentage obtained at the YK950 sample of 99.46%. The increase of calcination temperature tends to weight the percentage of $Nd_{1.2}FeO_3$ phase increased and decreased of Nd_2O_3 phase. This shows that the ions Nd_{+3} and Fe_{+3} forms of $NdFeO_3$ oxide material were improving without any impurity with increasing calcination temperature.

Table 2

Suitability (*figures-of-merit*) of Rietveld refinementof the samples

Samples	Profile (Rp)	Weighted Profile (Rwp)	The goodness of Fit (GoF(%))
YK750	4.57	6.06	0.9101
YK850	4.49	6.06	0.8726
YK950	4.73	6.15	0.9303

Table 3

Data output crystallographic Rietveld refinement of $NdFeO_3$ oxide material

Samples	a (Å)	b (Å)	c (Å)	V (Å^3)
YK750	5.581059 ± 0.000736	7.758627 ± 0.000947	5.448341 ± 0.000665	235.92
YK850	5.580203 ± 0.000695	7.756789 ± 0.000908	5.447646 ± 0.000626	235.79
YK950	5.580402 ± 0.000704	7.758957 ± 0.000919	5.449350 ± 0.000634	235.94

Table 4

The weight percentage of each phase in the samples using Rietica

Samples	Weight Percentage (%)			
	$NdFeO_3$ Phase	Error	Nd_2O_3 Phase	Error
YK750	99.07	1.00	0.93	0.10
YK850	99.18	0.96	0.82	0.96
YK950	99.46	0.96	0. 54	0.00

The results of structure visualization of $Nd_{1.2}FeO_3$ unit's cell based on lattice parameters have obtained from Rietveld refinement analysis described using software DIAMOND, as shown in Figures 6, 7, and 8, respectively. The orthorhombic crystal structure with the space group Pnma, in which grey spheres illustrate cation Nd_{+3}, green spheres represent cation Fe_{+3}, and the red spheres are oxygen ions with the Wyckoff of a position of each ion Nd_{+3} on (4c), ion Fe_{+3} in (4b) and ion O_2 (4c) and (8d). All lattice parameters *a, b,* and *c* are similar to each sample variation.

3.3. Scanning Electron Microscope (SEM) and Energy Dispersive Spectroscopy (EDS) Analysis

SEM was used as a method for analyzing the surface morphology of the $Nd_{1.2}FeO_3$ sample shown in Figures 9 and 10 with magnifications of 50,000x, and 100,000x, it can be seen that all samples have high homogeneity indicated by the morphology of the sample forming small uniform granules. These similar results also reported by Sujiono et al. [28]. The $Nd_{1.2}FeO_3$ sample, which is

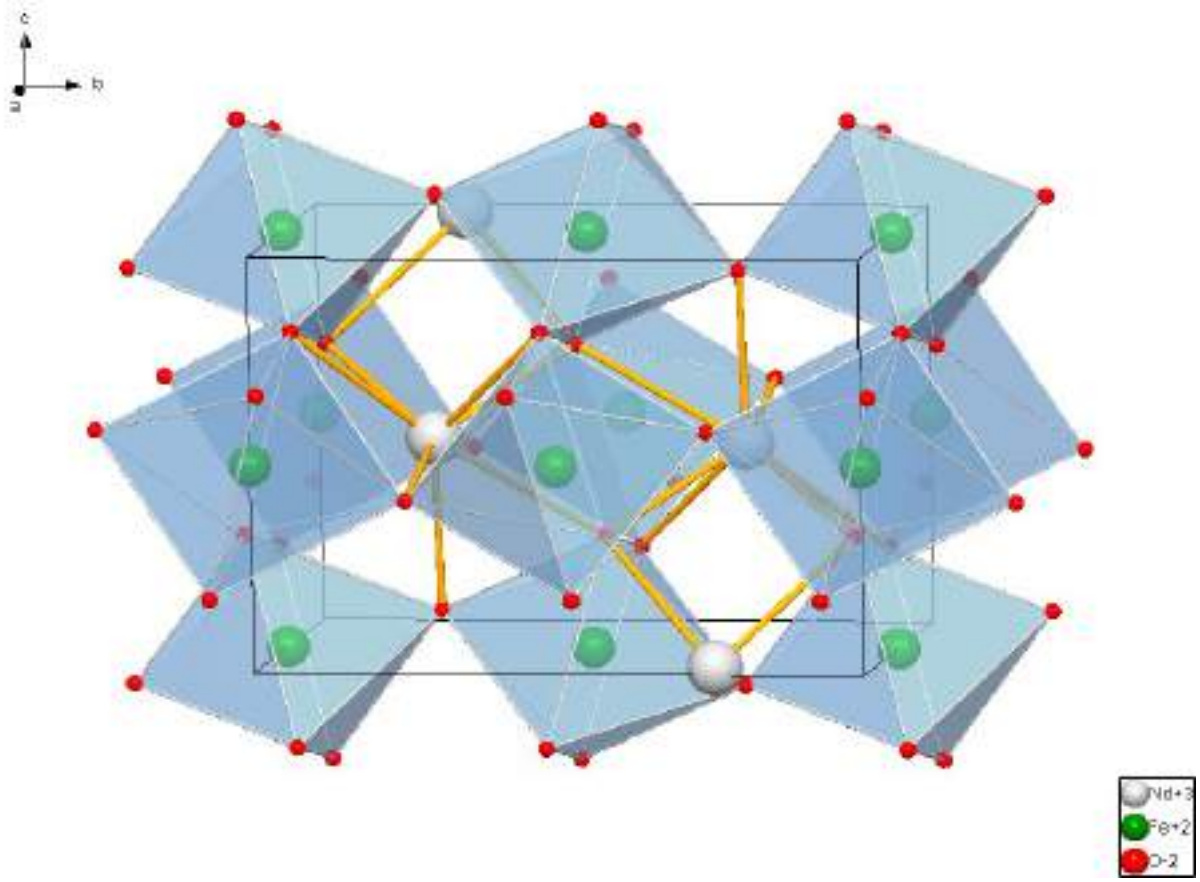

Fig. 6 - Visualization atomic structure of $NdFe_{1.2}O_3$ phase calcined at temperatures of 750ºC to the lattice parameter is a = 5.581059 ± 0.000736 Å, b = 7.758627 ± 0.000947 Å and c = 5.448341 ± 0.000665 Å.

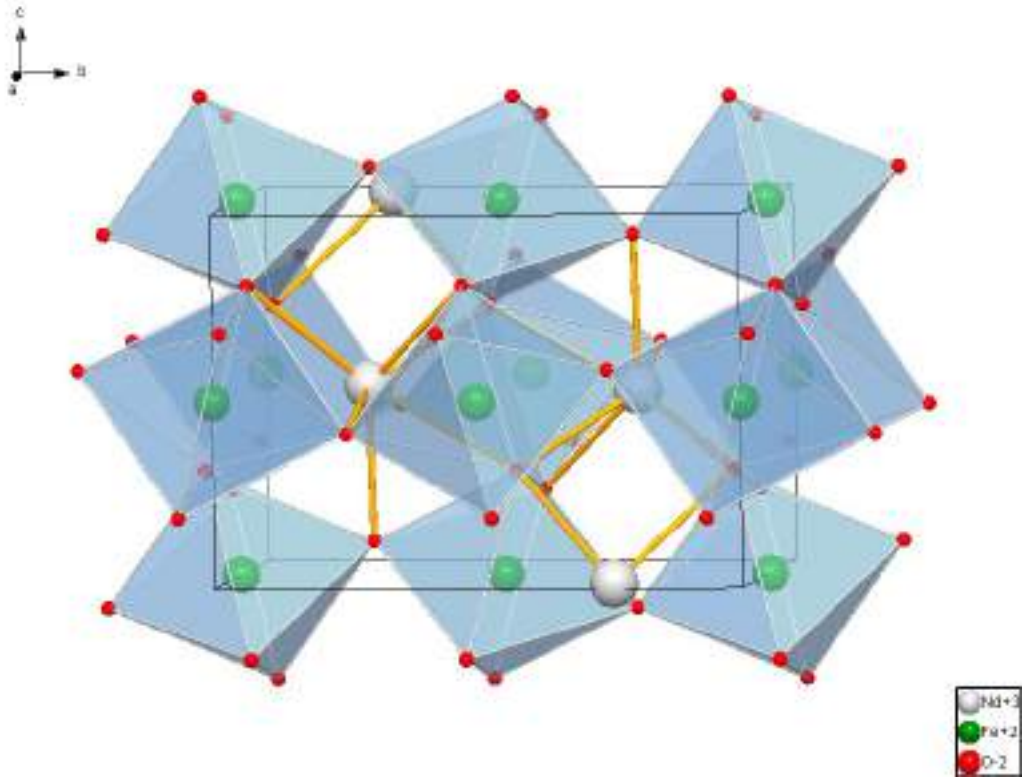

Fig. 7 - Visualization atomic structure of $NdFe_{1.2}O_3$ phase calcined at temperatures of 850ºC to the lattice parameter is a = 5.580203 ± 0.000695 Å, b = 7.756789 ± 0.000908 Å and c = 5.447646 ± 0.000626 Å.

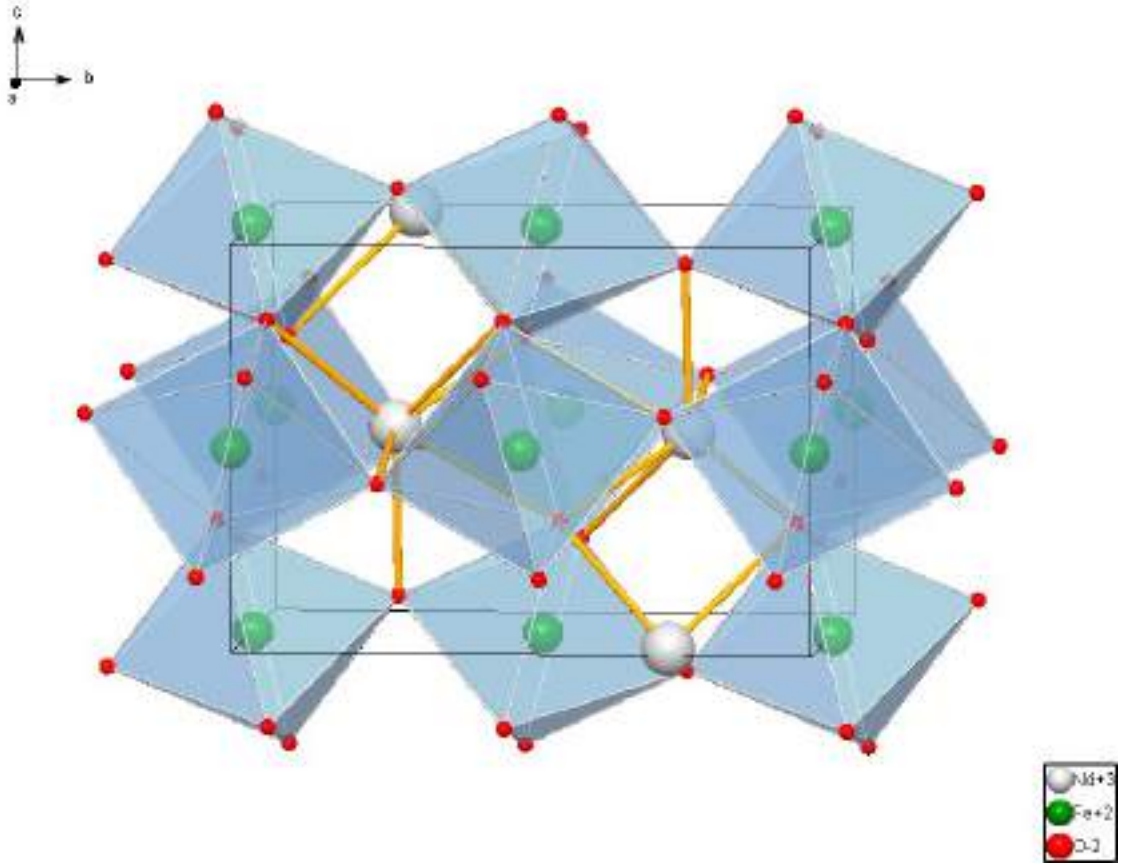

Fig. 8 - Visualization atomic structure of $NdFe_{1.2}O_3$ phase calcined at temperatures of 950ºC to the lattice parameter is a = 5.580402 ± 0.000704 Å, b = 7.758957 ± 0.000919 Å and c = 5.449350 ± 0.000634 Å.

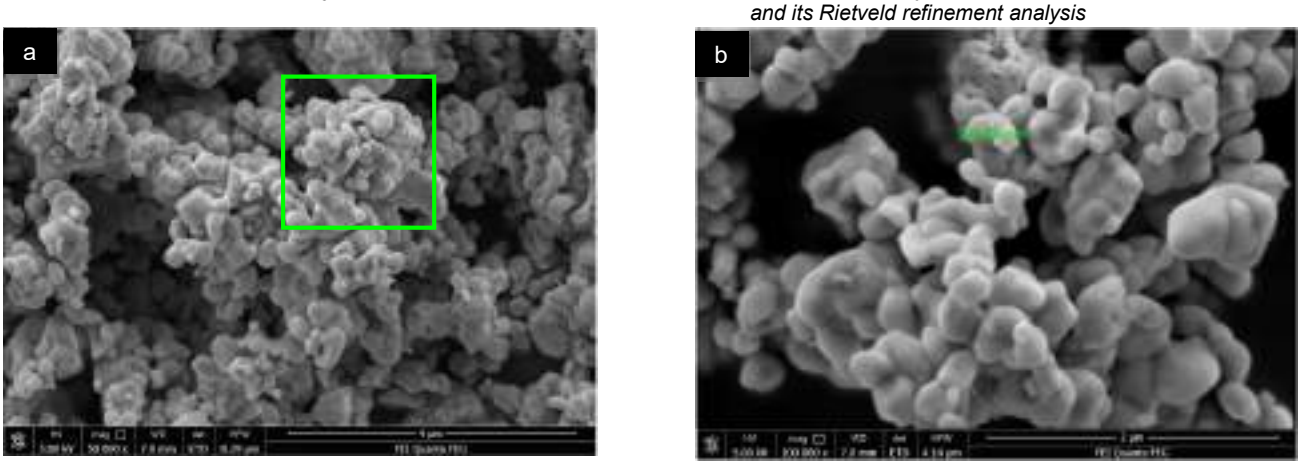

Fig. 9 - Morphology of sample $Nd_{1.2}FeO_3$ as a variation of calcination temperature YK750: a) Magnification 50,000x; b) Magnification 100,000x.

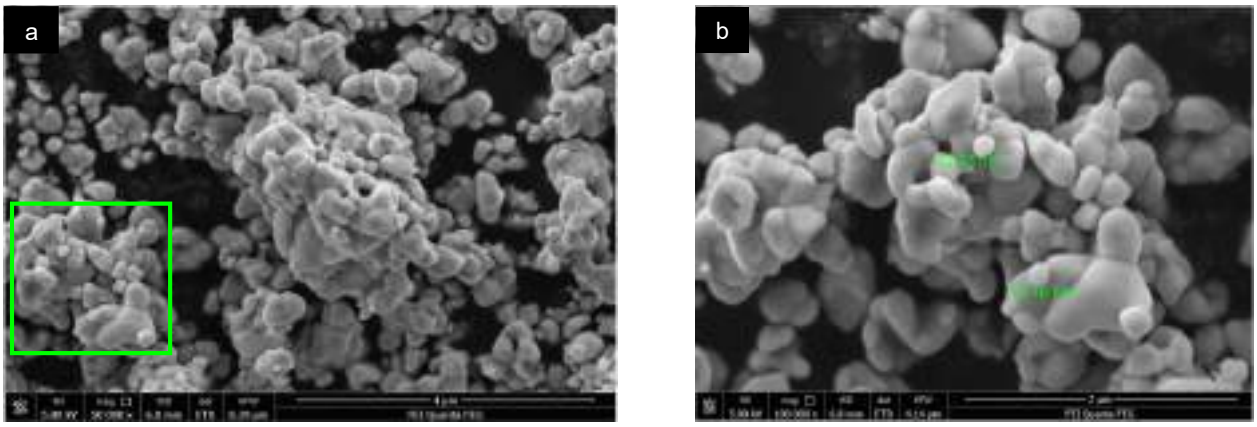

Fig. 10 - Morphology of sample $Nd_{1.2}FeO_3$ as a variation of calcination temperature YK950: a) Magnification 50,000x; b) Magnification 100,000x.

calcined at 750˚C, has a grain size 25.63 nm (Figures 9a) and the $Nd_{1.2}FeO_3$ sample, which is calcined at 950˚C has a grain size ranging from 14.16 nm – 22.93 nm (Figures 10b). The difference in grain size between the two samples is due to the calcination temperature. On the other terms of this powder has a high porosity so that it becomes one of the advantages to improve its characteristics as a gas sensor [3].

Furthermore, the EDS, it has confirmed that consistently form Nd, Fe, O with an average stoichiometric ratio of 1.2: 1: 3 which contained Nd (53.90 wt%), Fe (26.49 wt%), O (15.09 wt%), C (4.52 wt%), and Nd (49.81 wt%), Fe (23.23 wt%), O (16.80 wt%), C (10.16 wt%) respectively as shown in Table 5.

Elemental maps of the $Nd_{1.2}FeO_3$ samples surface area are shown in Figures 11 and 12, respectively. Figures 11a and 12a contain a secondary electron (SE) image of the $Nd_{1.2}FeO_3$ samples as well as the corresponding maps of the distribution of chemical elements on the scanned surface. The elemental mapping of the $Nd_{1.2}FeO_3$ samples shows that the surface area was rich with neodymium (in neodymium-rich area, see Nd-MAB map), iron (in iron-rich area, see Fe-K map), and oxygen (see O-K map), respectively. The presence of carbon in EDS results is origin from carbon adhesive tape. There are no impurities seen, and it can be confirmed that the results of the XRD and SEM-EDS analyzes were consistent with the dominant peak of hkl 121 [10,11].

Table 5
The elemental composition of element $Nd_{1.2}FeO_3$ phase using EDS

Element	Norm. C [wt%]	
	YK 750	YK950
Nd	53.90	49.81
Fe	26.49	23.23
O	15.09	21.35
C	4.52	12.92

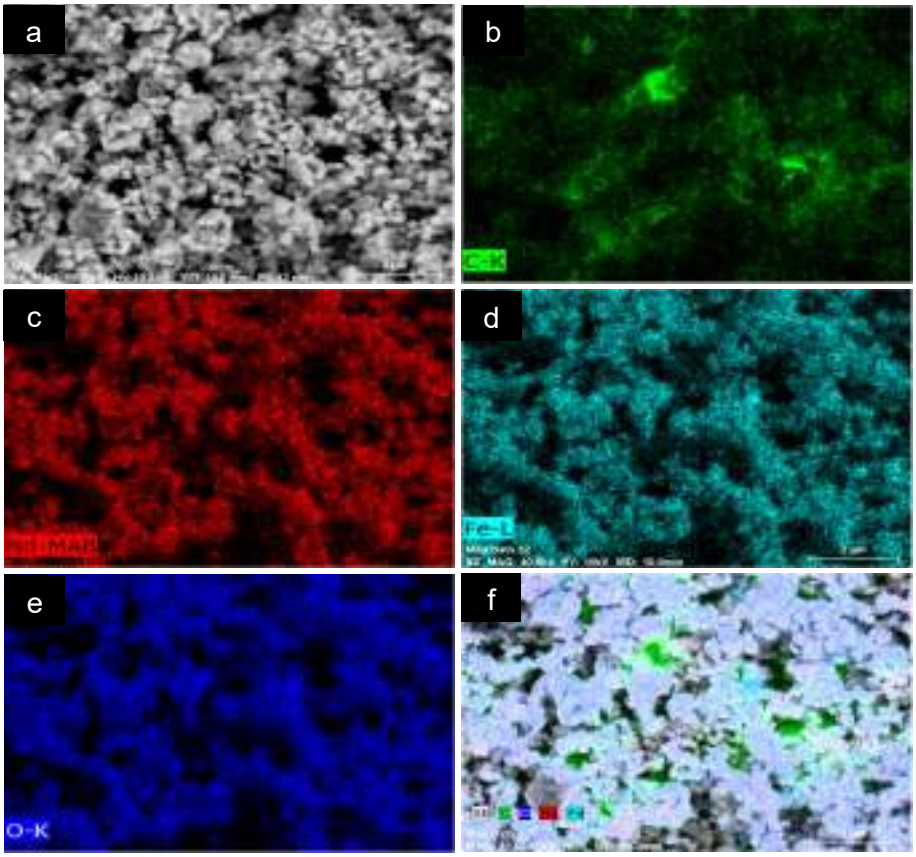

Fig. 11 – Analysis fast mapping EDS of sample $Nd_{1.2}FeO_3$: a) SE Image, b) EDS mapping of carbon, c) neodymium, d) iron, e) oxygen, and f) EDS mapping for all elements combined as a variation of calcination temperature YK750.

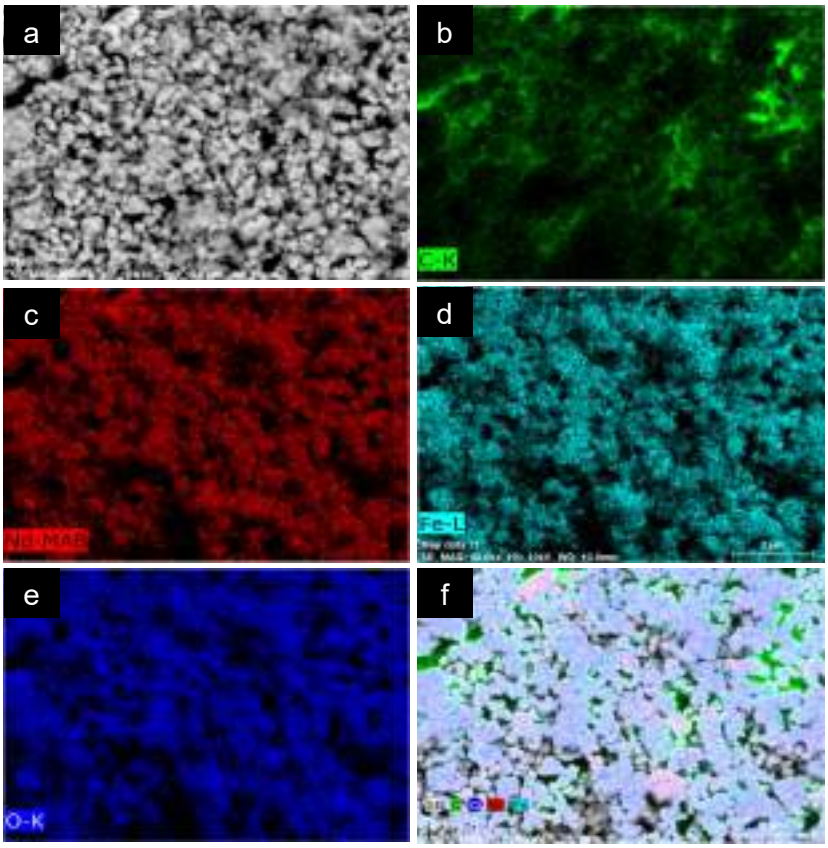

Fig. 12 - Analysis fast mapping EDS of sample $Nd_{1.2}FeO_3$: a) SE Image, b) EDS mapping of carbon, c) neodymium, d) iron, e) oxygen, and f) EDS mapping for all elements combined as a variation of calcination temperature YK950.

4.Conclusion

$Nd_{1.2}FeO_3$ oxide material has successfully synthesized as a basis of the material gas sensor. The results of X-ray diffraction analysis showed $NdFeO_3$ and Nd_2O_3 phase, in which the crystal structure of the phase $Nd_{1.2}FeO_3$ is orthorhombic to the space group Pnma. $NdFeO_3$ phase lattice constant for each sample is YK750 a = 5.581059 ± 0.000736 Å, b = 7.758627 ± 0.000947 Å, c = 5.448341 ± 0.000665 Å; YK850 a = 5.580203 ± 0.000695 Å, b = 7.756789 ± 0.000908 Å, c = 5.447646 ± 0.000626 Å; and YK950 a = 5.580402 ± 0.000704 Å, b = 7.758957 ± 0.000919 Å, c = 5.449350 ± 0.000634 Å, respectively related to the GoF values <1% and the estimated size of the crystals is 372 nm. In the analysis of surface area data and elemental compositions confirmed that $Nd_{1.2}FeO_3$ samples have homogeneous morphology and grain sizes that tend to be uniform.

Acknowledgments
This research was funded by Directorate Research and Community Services, Ministry of Research and Technology, Republic of Indonesia, under the research scheme of fundamental research.

REFERENCES

[1] N. Q. Minh, Ceramic Fuel Cells, J. Am. Ceram. Soc. 1993, **76**(3), 563-583.
[2] M. Siemons, U. Simon, Preparation and gas sensing properties of nanocrystalline La-doped $CoTiO_3$, Sens. Actuators B Chem. 2006, **120**(1), 110-118.
[3] T. G. Ho, T. D. Ha, Q. N. Pham, H. T. Giang, Do. T. A. Thu, N. T. Nguyen, Nanosized perovskite oxide $NdFeO_3$ as material for a carbon-monoxide catalytic gas sensor, Adv. Nat. Sci: Nanosci. Nanotechnol. 2011, **2**(1), 015012.
[4] X. Niu, H. Li, G. Liu, Preparation characterization and photocatalytic properties of $REFeO_3$ (RE = Sm, Eu, Gd), J. Mol. Catal. A-Chem. 2005, **232**(1-2), 89-93.
[5] M. A. Pena, J. L. G. Fierro, Chemical Structures and Performance of Perovskite Oxides, Chem. Rev., 2001, **101**(7), 1981-2018.
[6] X. Li, C. Tang, M. Ai, L. Dong, Z. Xu, Controllable Synthesis of Pure-Phase Rare-Earth Orthoferrites Hollow Spheres with a Porous Shell and Their Catalytic Performance for the CO + NO Reaction, Chem. Mater. 2010, **22**(17), 4879-4889.
[7] R. Przenioslo, I. Sosnowska, M. Loewenhaupt, A. Taylor, Crystal field excitations of $NdFeO_3$, J. Magn. Magn. Mater. 1995, **140-144**(3), 2151-2152.
[8] E. H. Sujiono, A. C. M. Said, M. Y. Dahlan, R. A. Imran, S. Samnur, Refinement Analysis using the Rietveld Method of $Nd_{1.2}Fe_1O_3$ Oxide Material Synthesized by Solid-State Reaction, J. Nano- Electron. Phys. 2018, **10**, 02034.
[9] A. Bashir, M. Ikram, R. Kumar, P. Takur, K. H. Chae, W. K. Choi, V. R. Reddy, Structural, magnetic, and electronic structure studies of $NdFe_{1-x}Ni_xO_3$, J. Phys. Condens. Matter, 1993, **21**, 325501.
[10] N. Xinshu, D. Weimin, K. Jiang, Preparation and Gas-Sensing Properties of $NdFeO_3$ Nanocrystalline, J. Rare Earths, 2003, **21**, 630-632.
[11] X. Lou, X. Jia, J. Xu, Preparation, and gas sensing property for C_2H_5OH detection of perovskite-type $NdFeO_3$, J. Rare Earths, 2005, **23**, 328-331.
[12] W. Zheng, R. Liu, D. Peng, G. Meng, Hydrothermal synthesis of $LaFeO_3$ under carbonate-containing medium, Mater. Lett. 2000, **43**, 19-22.
[13] S. S. Manoharan, K. C. Patil, Combustion route to fine particle perovskite oxides, J. Solid State Chem. 1993, **102**, 267-267.
[14] A. Chakraborty, P. S. Devi, H. S. Maiti, Low temperature synthesis, and some physical properties of barium-substituted lanthanum manganite ($La_{1-x}Ba_xMnO_3$), J. Mater. Res. 1995, **10**, 918-925.
[15] H. Cui, M. Zayat, D. Levy, Epoxide assisted the sol-gel synthesis of perovskite-type $LaM_xFe_{1-x}O_3$ (M = Ni, Co) nanoparticles, J. Non-Cryst. Solids, 2006, **352**, 3035-3040.
[16] H. N. Pandya, R. G. Kulkarni, P. H. Parsania, Study of cerium orthoferrite prepared by wet chemical method, Mat. Res. Bull. 1990, **25**, 1073-1077.
[17] S. Singh, B. C. Yadav, P. K. Dwivedi, Fabrication of nanobeads structured perovskite-type neodymium iron oxide film: its structural, optical, electrical, and LPG sensing investigations, Sens. Actuators B-Chem. 2013, **177**, 730-739.
[18] L. Smart, E. Moore, Solid State Chemistry, Fourth. Ed., CRC Handbook, Boca Raton: CRC Press, UK, 2005.
[19] E. H. Sujiono, R. A. Sani, T. Saragi, P. Arifin, M. Barmawi, Thin Films Deposited by MOCVD Vertical Reactor with a Flow Guide, Phys. Status Solidi A, 2001, **187**, 471-479.
[20] E. H. Sujiono, H. Ahmad, F. Rera, S. Samnur, Crystal Structure, and Morphology Analysis of $Nd_{1+x}Ba_{2-x}Cu_3O_7$ Oxide Alloy Surface Developed by Solid-State Reaction Method. J. Fis. dan Appl. 2011, **7**, 110101.
[21] E. H. Sujiono and Muharram, $Nd_1(Fe)_xBa_{2-x}Cu_3O_y$ Oxide Material and Its Synthesis Method (in Indonesian), ID Patent No. IDP000044179, January 23, 2017.
[22] H. M. Rietveld, Line profiles of neutron powder-diffraction peaks for structure refinement, Acta Cryst. 1967, **22**, 151-152.
[23] V. A. Streltsov, N. Ishizawa, Synchrotron X-ray study of the electron density in $RFeO_3$ (R = Nd, Dy), Acta Crystallogr. Sec., 1999, B. **55**, 1-7.
[24] S. Geller, E. Wood, Crystallographic studies of perovskite-like compounds, I. Rare earth orthoferrites and $YFeO_3$, $YCrO_3$, $YAlO_3$, Acta Cryst. 1956, **9**, 563-568.
[25] W. Sławin´ski, R. Przeniosło, I. Sosnowska, E. Suard, Spin reorientation and structural changes in $NdFeO_3$, J. Phys. Condens. Matter, 2005, **17**, 4605.
[26] V. Zharvan, Y. N. I. Kamaruddin, S. Samnur, E. H. Sujiono, The Effect of Molar Ratio on Crystal Structure and Morphology of $Nd_{1+x}FeO_3$ (X=0.1, 0.2, and 0.3) Oxide Alloy Material Synthesized by Solid-State Reaction Method, IOP Conf. Ser.: Mater. Sci. Eng. 2017, **202**, 012072.
[27] S. A. Mir, M. Ikram, K. Asokan, Structural, optical, and dielectric properties of Ni substituted $NdFeO_3$, Optik, 2014, **125**, 6903-6908.
[28] E. H. Sujiono, M. Y. Dahlan, R. A. Imran, A. C. M. Said, S. Samnur, The Effect of Calcination Temperature on Crystal Structures and Morphologies of $Nd_{1.2}FeO_3$ Synthesized by Solid-State Reaction, IOP Conf. Ser.: Mater. Sci. Eng. 2018, **367**, 012042.
[29] E. H. Sujiono, A. C. M. Said, M. Y. Dahlan, R. A. Imran, S. Samnur, Influence of Annealing Time Variation on Crystal Structure and Morphology of Oxide Material $Nd_{1.2}FeO_3$ by Solid-State Reaction Method, IOP Conf. Ser.: Mater. Sci. Eng. 2018, **367**, 012037.
[30] E. H. Sujiono, V. Zharvan, M. Y. Dahlan, A. C. M. Said, J. Agus, S. Samnur, Study on Morphology and Crystal Structure of Pd Doped $Nd_{1.2}FeO_3$, Materials Today: Proceedings, 2019, **13**, 258-263.
[31] Y. Wang, S. Cao, M. Shao, S. Yuan, B. Kang, J. Zhang, A. Wu, J. Xu, Growth rate dependence of the $NdFeO_3$ single crystal grown by float-zone technique, J. Cryst. Growth, 2011, **318**, 927-931.
[32] S. Chanda, S. Saha, A. Dutta, T. P. Sinha, Raman spectroscopy, and dielectric properties of nanoceramic $NdFeO_3$, Mat. Res. Bull. 2013, **48**, 1688-1693.
[33] H. Aono, K. Kinoshita, M. Sakamoto, Y. Sadaoka, Characterizations of $NdFe_{0.5}Co_{0.5}O_3$ Trimetallic Oxide Prepared by Thermal Decomposition of Heteronuclear Complex, $Nd[Fe_{0.5}Co_{0.5}(CN)6]\cdot 4H_2O$, J. Ceram. Soc. Jpn. 1998, **106**, 10.
[34] M. Buschbaum, Zur Struktur der A-Form der Sesquioxide der Seltenen Erden II Strukturuntersuchung an Nd_2O_3, Z. Anorg. Allg. Chem. 1998, **343**, 6-10.
[35] E. H. Kisi, Rietveld Analysis of Powder Diffraction Patterns. Mater. Forum, 1994, **18**, 135-155.
[36] J. Shanker, M. B. Suresh, D. S. Babu, Synthesis Characterization and Electrical Properties of $NdXO_3$(X=Cr, Fe) Nanoparticles, Mater. Today Proc. 2016, **3**, 2091-2100.

****